



SAR IMAGE PROCESSING FOR CROP MONITORING

Anne Orban, Dominique Derauw, and Christian Barbier

Centre Spatial de Liège – Université de Liège

cbarbier@ulg.ac.be

Agriculture and Vegetation at a Local Scale

Habay-La-Neuve, 20 September 2005



CONTENTS

I. CONTEXT

To present **advanced SAR processing techniques** potentially applicable to crop monitoring :

II. InSAR

II.1 Basic Principles

II.2 Sample Results

III. PolSAR

III.1 Basic Principles

III.2 Sample Results

IV. PolInSAR

IV.1 Basic Principles

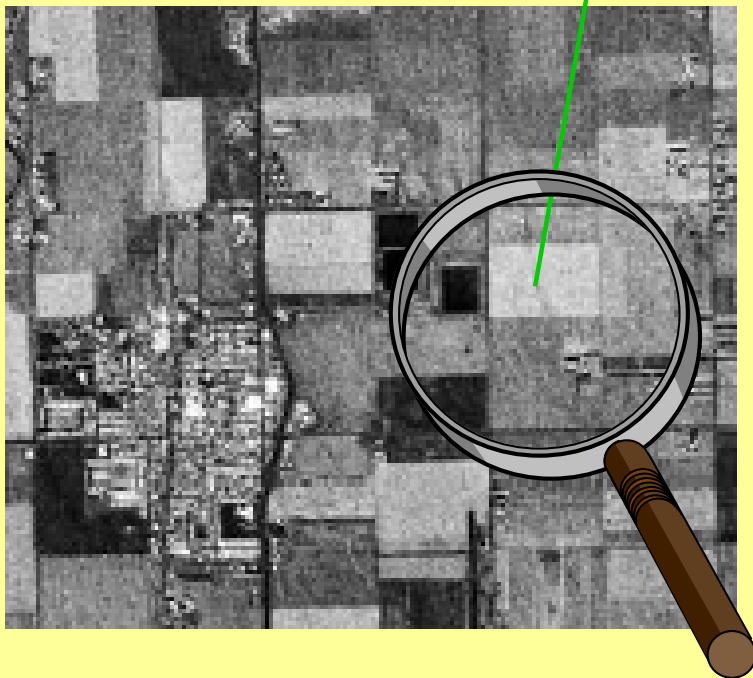
IV.2 A Picture Book Example

V. CONCLUSIONS AND PERSPECTIVES



I. CONTEXT

$$pixel = \underbrace{A}_{\substack{\text{amplitude} \\ \text{SAR}}} \exp(j \underbrace{\phi}_{\substack{\text{phase} \\ \text{InSAR}}}) \underbrace{\vec{p}}_{\substack{\text{polarisation state} \\ \text{PolSAR}}} \\ \underbrace{\hspace{15em}}_{\text{PolInSAR}}$$





II. InSAR

Projects :

TELSAT Project T3/12/012 « Demonstration and Evaluation of SAR Interferometry » (1993-1995)

CSL

ERS Tandem Project B302 « An Assessment of SAR Phasimetry by Case Studies in Tectonics and Agronomy » (1997-1998)

CSL, FUSAGx, CRA, UCL-MILA, ULg-LGT

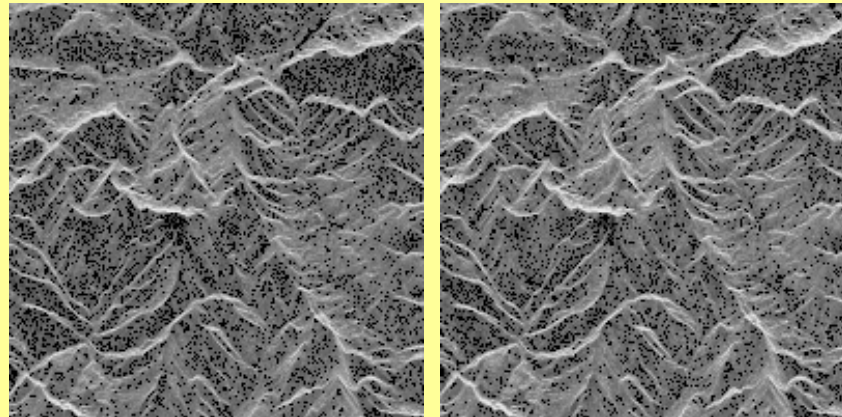
STEREO Project SR/00/01 « Modelling Crop Growth Based on Hydrology and Assimilation of Remotely Sensed Data » (2001-2006)

UCL, UGent, CSL

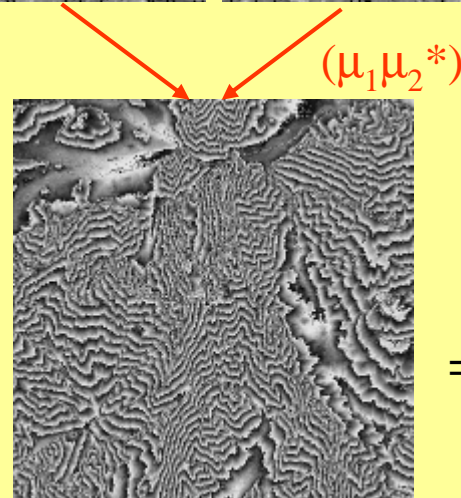


II.1 InSAR : Basic Principles

Pass 1
(μ_1)



Pass 2
(μ_2)



($\mu_1 \mu_2^*$)

**Interference pattern
==> Topography, terrain and
atmospheric changes**



II.2 InSAR : Sample Results

InSAR Coherence for Crop Parameters Monitoring

Xavier Blaes¹, Pierre Defourny¹, Dominique Derauw² and Christian Barbier²

¹ Department of Land Use Planning, College of Agriculture, Université Catholique de Louvain
Place Croix du Sud, 2/16 - 1348 Louvain-la-Neuve, Belgium

Phone : +32 10/ 47 81 92, Fax: +32 10/ 47 88 98, email: blaes@biomucl.ac.be, <http://www.agro.ucl.ac.be/biom/>

² Centre Spatial de Liège, Université de Liège, Avenue du Pré-Aily - 4031 ANGLEUR, Belgium
Phone : +32 4 / 367 66 68 Fax : +32 4 / 367 56 13 <http://www.ulg.ac.be/cshulg/>

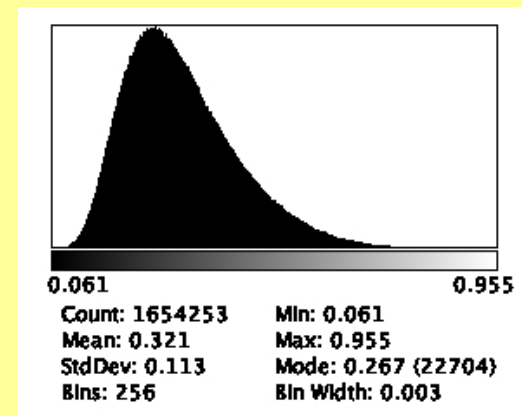
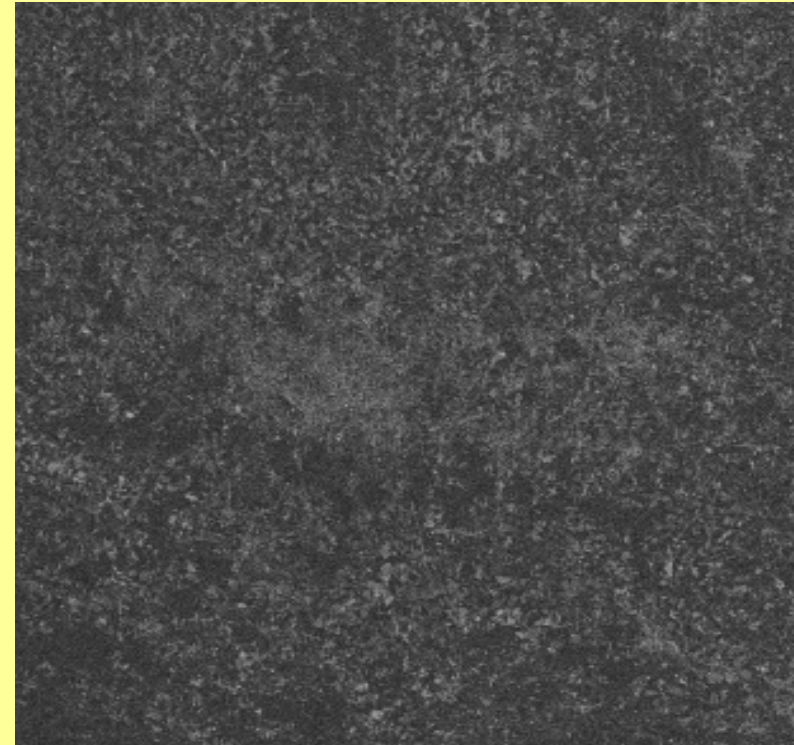
**Proc. FRINGE'99 Symp., Liège 10-12 Nov. 1999,
ESA SP-478**



Basic Product : the Coherence Map

$$\gamma = \frac{|\langle \mu_1 | \mu_2^* \rangle|}{\sqrt{\langle \mu_1 | \mu_1^* \rangle \langle \mu_2 | \mu_2^* \rangle}}$$
$$= \gamma_{SNR} \gamma_{Baseline} \gamma_{Temporal}$$

**(ERS acquisition over Belgium:
region of Charleroi - 03 & 04/1996
Interferometric baseline = 330 meters)**



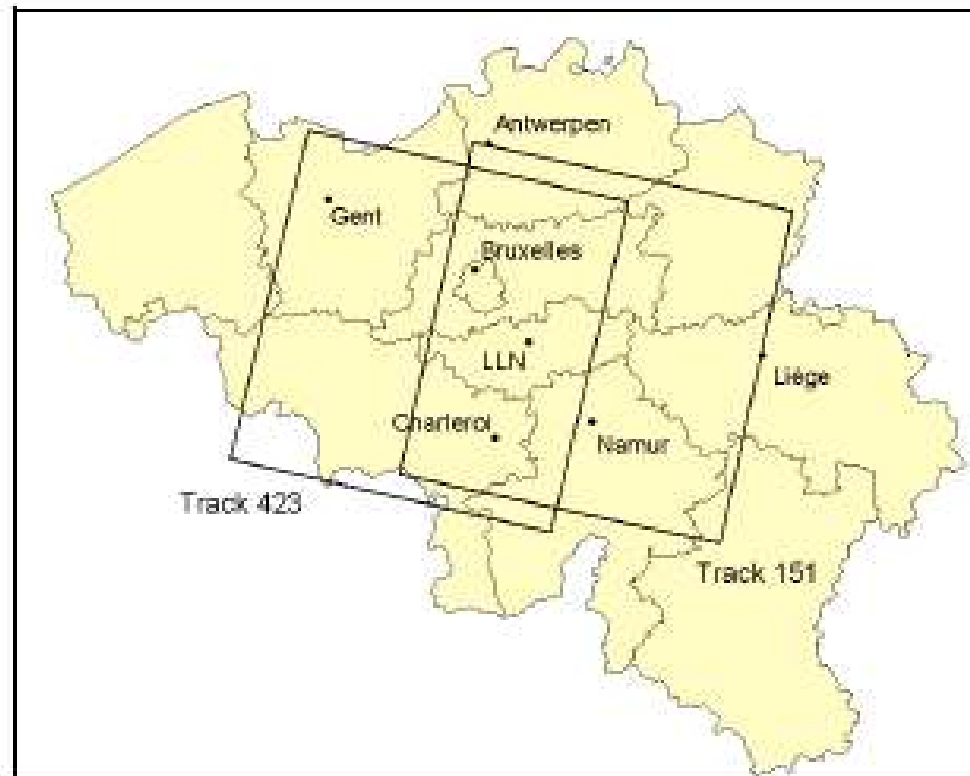


Figure 1: Localisation of the two set of images over the study area.



Strong relationships between the plant height and the coherence are observed for the 4 crops. A prediction model of the wheat height has been computed and the mean absolute error of about 7 cm seems compatible with the information requirements for a crop monitoring systems. The shape of these relationships varies according to the crop structure and their respective development type.

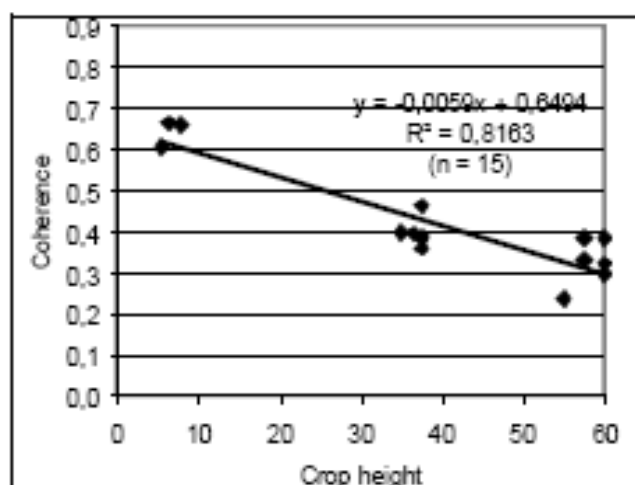


Figure 7: Linear regression between the tandem coherence and the potato height.

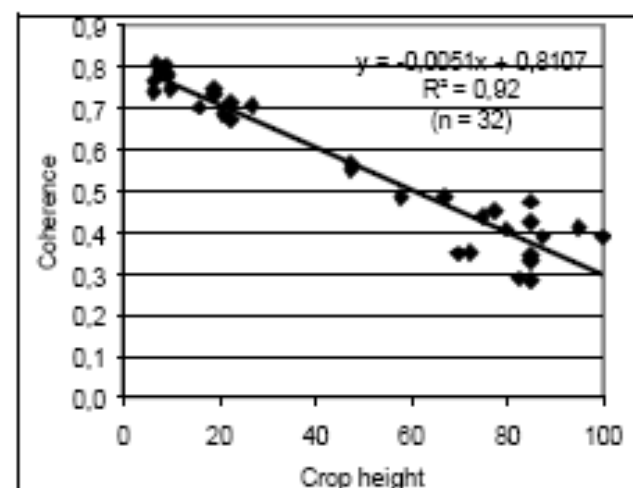


Figure 5: relationship between the tandem coherence and the winter wheat height.



III. PolSAR

Projects :

**Project SA/12/001 « Development of a SAOCOM SAR Processor»
(2000 - 2008)**

CSL, SPACEBEL

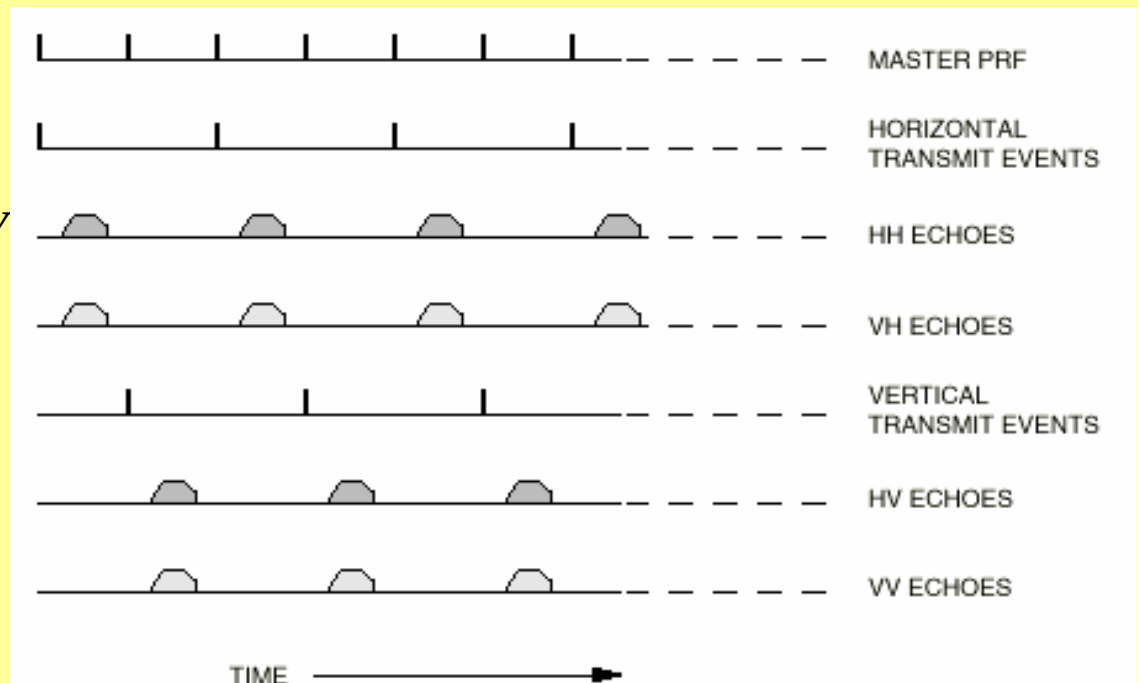
**STEREO Project SR/00/01 « Modelling Crop Growth Based on
Hydrology and Assimilation of Remotely Sensed Data » (2001-2006)**

UCL, UGent, CSL



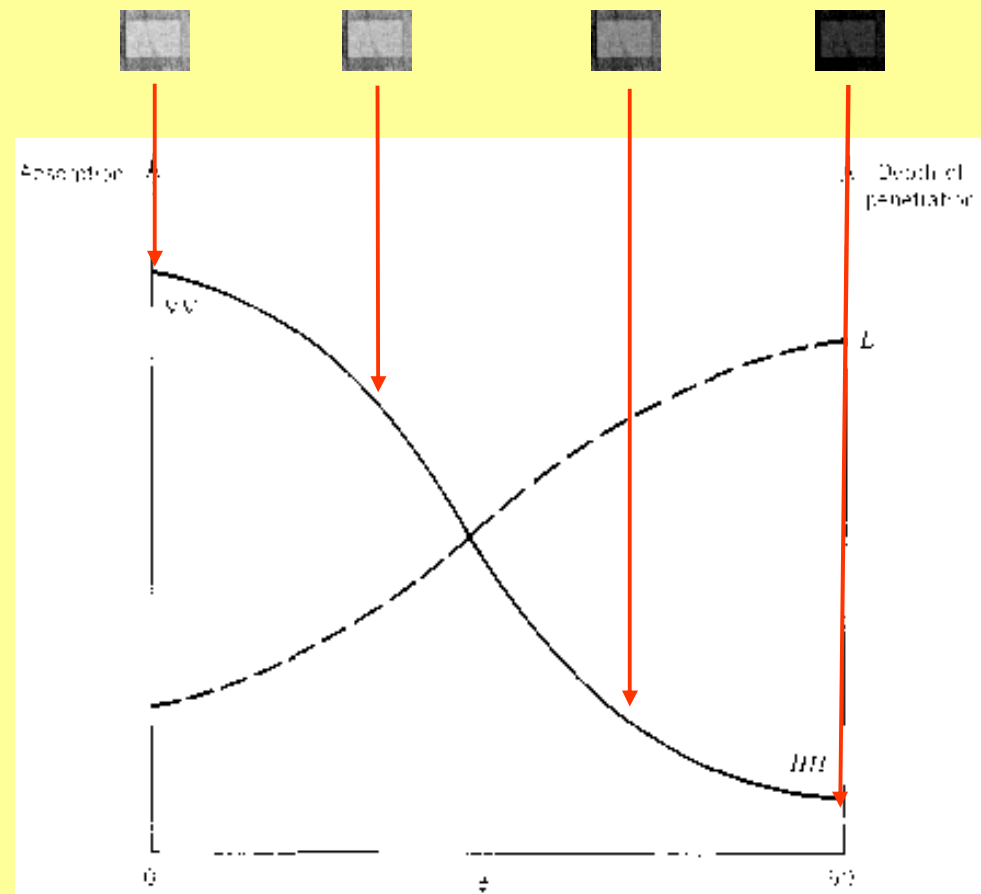
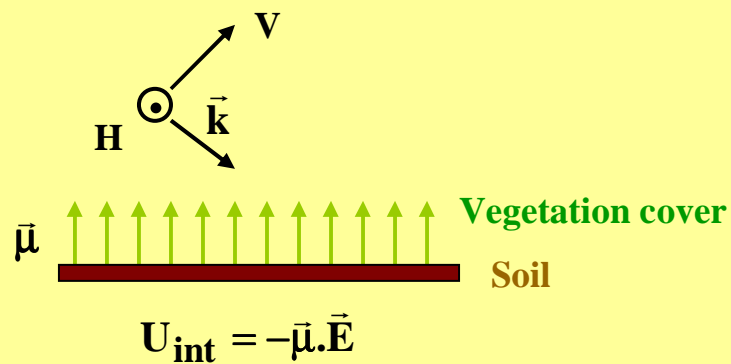
III.1 PolSAR : Basic Principles

- **Single-polarization mode**
 - transmit in 1 single linear polarization: H or V
 - receive in the same polarization
 - 1 acquisition: **HH** or **VV**
- **Dual-polarization mode**
 - transmit in H or V
 - receive in H and V
 - 2 acquisitions: **HH/HV** or **VV/HV** or **HH/VV**
- **Quad-polarization mode**
 - transmit alternatively H and V
 - receive in H and V
 - 4 acquisitions: **HH HV VH VV**





PolSAR provides **scattering mechanisms information**.





III.2 PolSAR : Sample Results

Polarimetric Processor

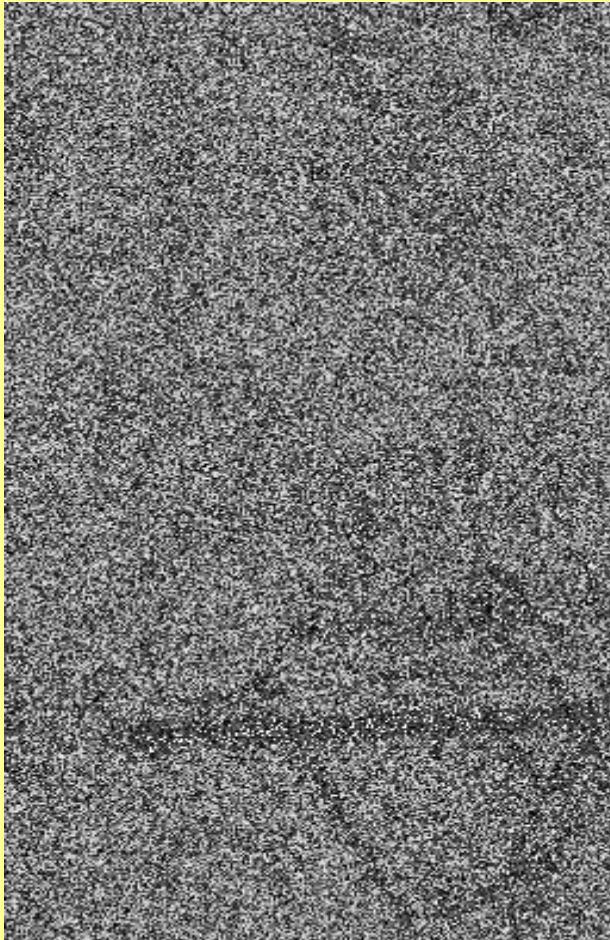
→ Input: images produced by the SAR processor

- **Backscattering coefficient images σ°**
- **Quad-polarimetric processor**
- **Dual-polarimetric processor**

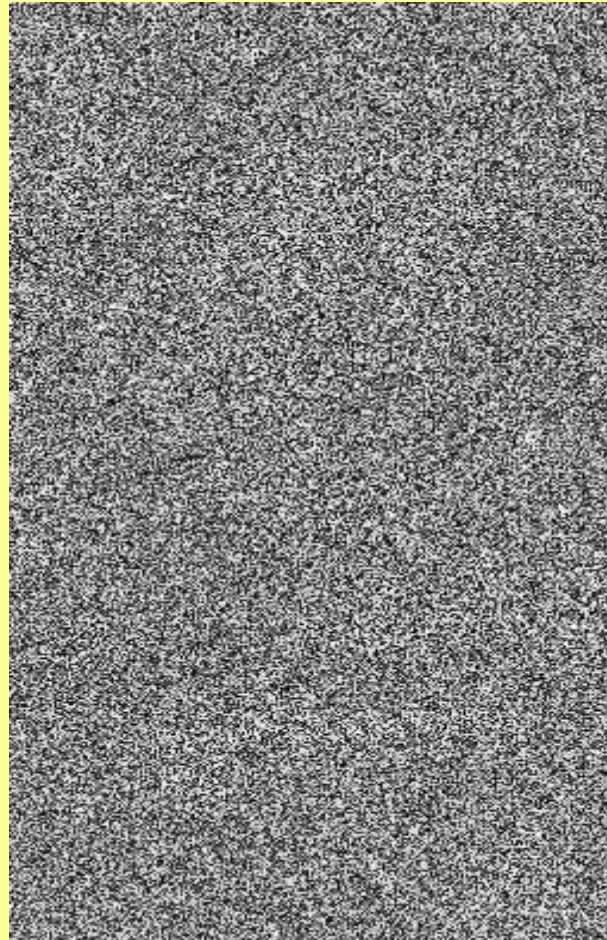


1. Backscattering Coefficient Images

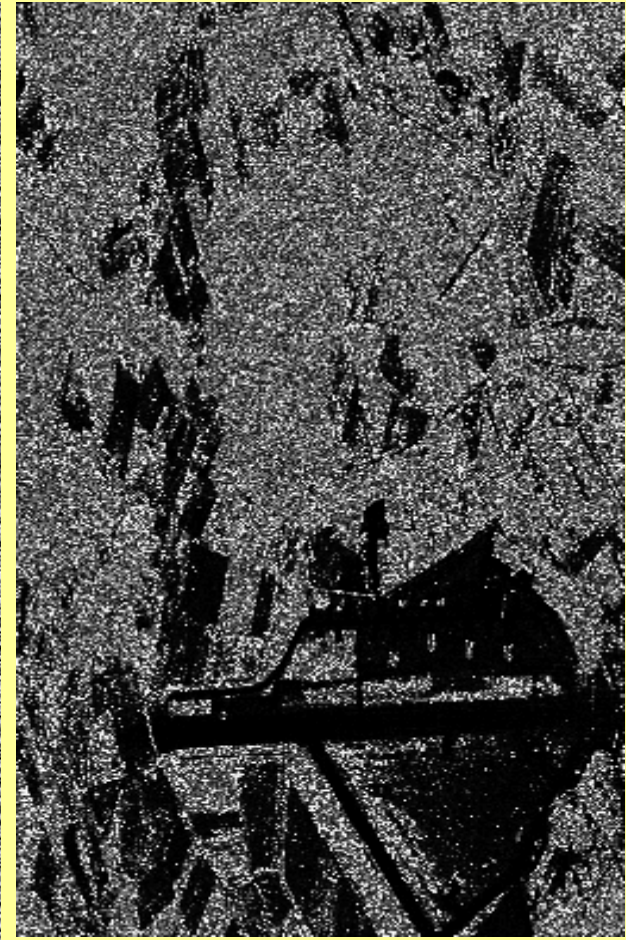
σ°_{VV}



σ°_{HH}



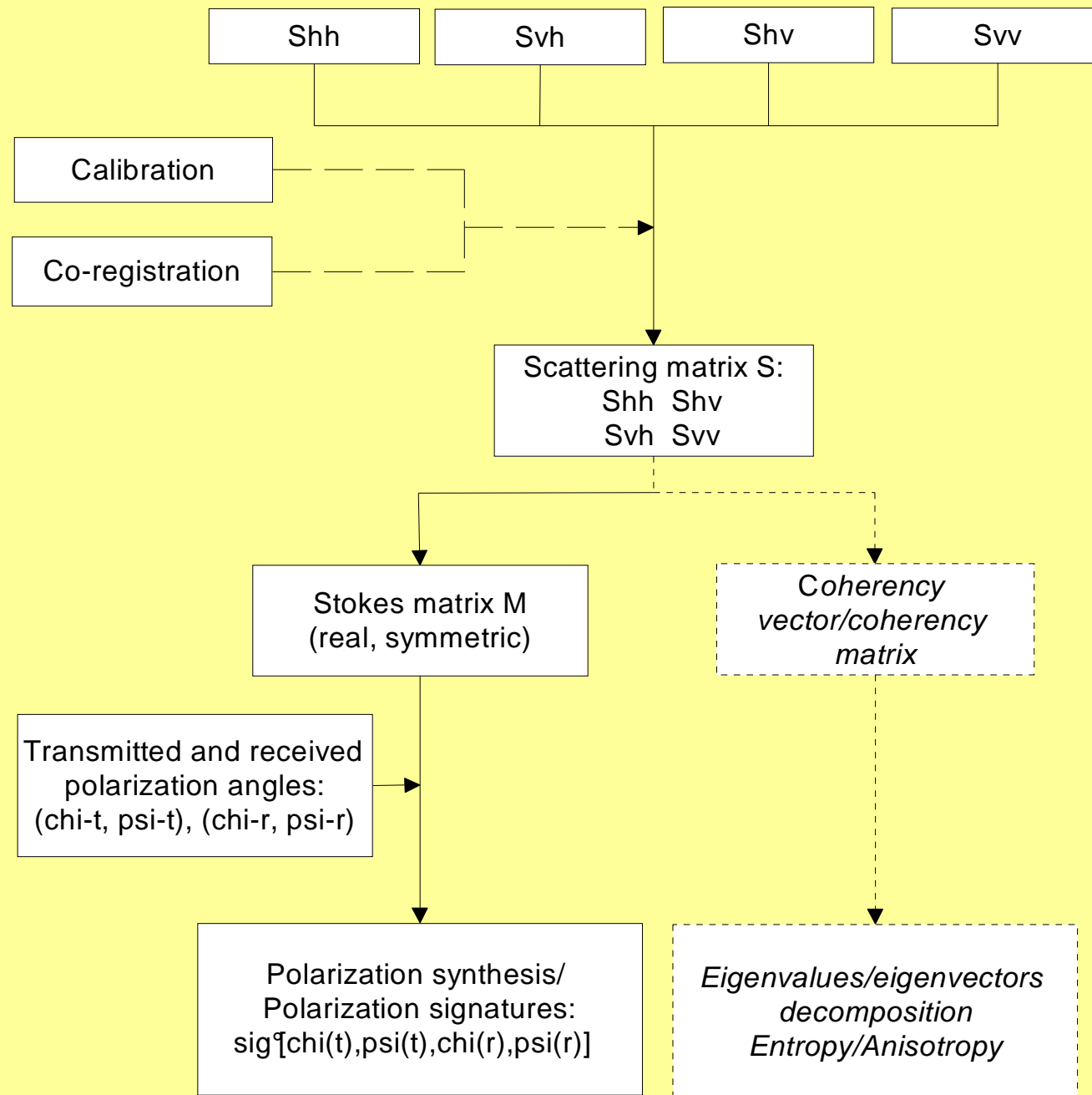
σ°_{HV}



All the images presented here have been produced at CSL, using polarimetric data provided by the DLR



2. Quad-Polarimetric Processor





Decomposition H/A/ α

H



α



A



$$H = -\sum_{i=1}^3 P_i \log_3(P_i)$$

$$P_i = \frac{\lambda_i}{\sum \lambda_i}$$

α target scattering type $[0^\circ, 90^\circ]$

$$A = \frac{\lambda_2 - \lambda_3}{\lambda_2 + \lambda_3}$$

Classification methods based on **scattering mechanisms**:

urban areas, forests, vegetated/non-vegetated, clear-cut, water/ice surfaces...

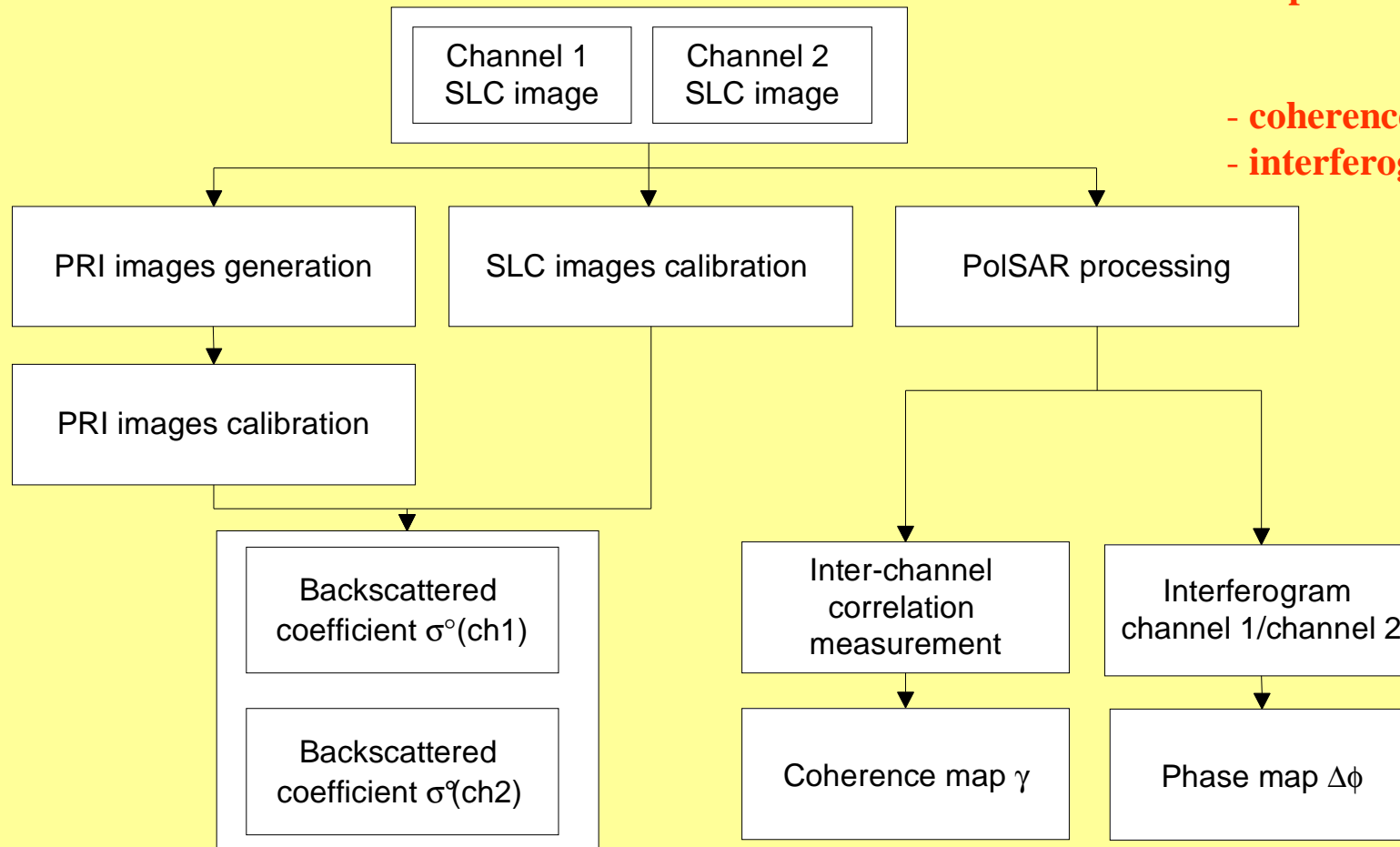


3. Dual-Polarimetric Processing

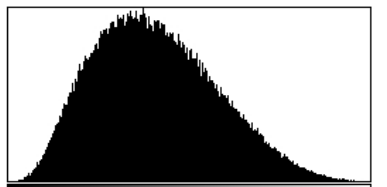
2 measurements: HH/HV or VV/HV

→ no polarization synthesis

→ no decomposition algorithm



↓
- coherence analysis
- interferogram



Count: 178861 Min: 0.089
Mean: 0.457 Max: 0.992
StdDev: 0.152 Mode: 0.425 (1642)
Bins: 256 Bin Width: 0.004



Coherence HH/VV



Interferogram HH/VV



IV. PolInSAR

Project :

**STEREO Project SR/00/53 «Polarimetric SAR Interferometry »
(2001-2006)**

CSL, UCL, RMA



IV.1 PolInSAR : Basic Principles

PolInSAR = vector InSAR

InSAR → height information

PolSAR → scattering mechanisms information

PolInSAR → height distribution of scattering mechanisms



IV.2 PolInSAR : A Picture Book Example

**S.R. Cloude and K.P. Papathanasiou,
“Polarimetric SAR Interferometry”,
IEEE Trans. Geosci. Remote Sensing 36(5), 1551-1656 (Sept. 1998)**



Fig. 1. SAR images of the test area across the Selenga delta at SE Lake Baikal. (Tien Shan test site, latitude N 52.16°, longitude E 106.67°). (a) Total power image, (b) *HH* image, and (c) *LL* image.



The Coherence Maps

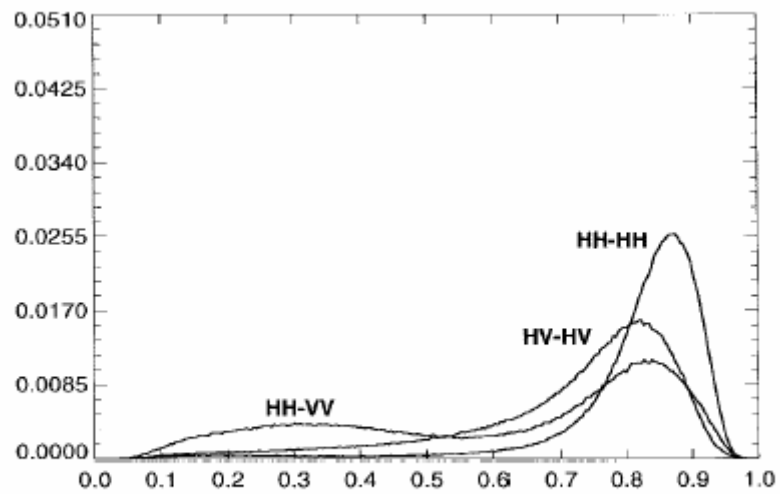


Fig. 3. Coherence histograms in the (H, V) -polarization basis.

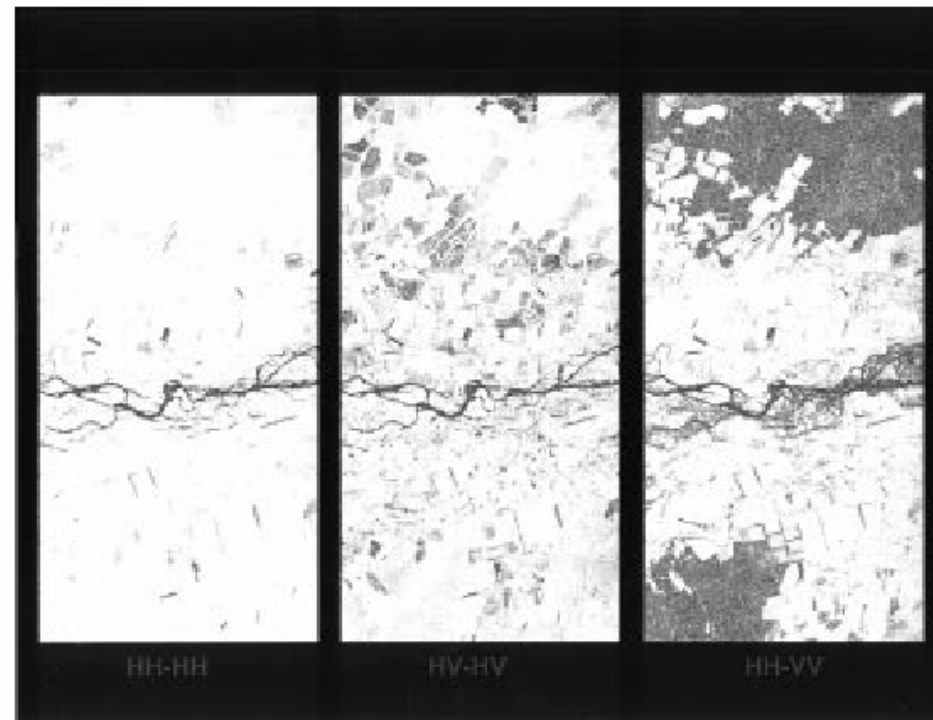


Fig. 2. Coherence maps of interferograms in the (H, V) -polarization basis (Left: $HH-HH$. Middle: $HV-HV$. Right: $HH-VV$).



Decomposition Into Coherence-Optimized States

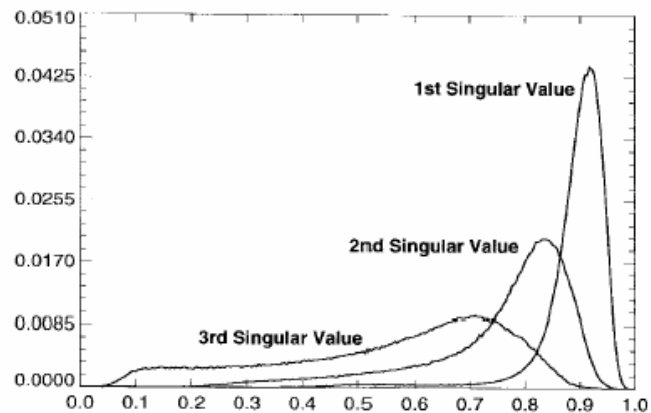


Fig. 6. Coherence histograms of the optimized interferograms.

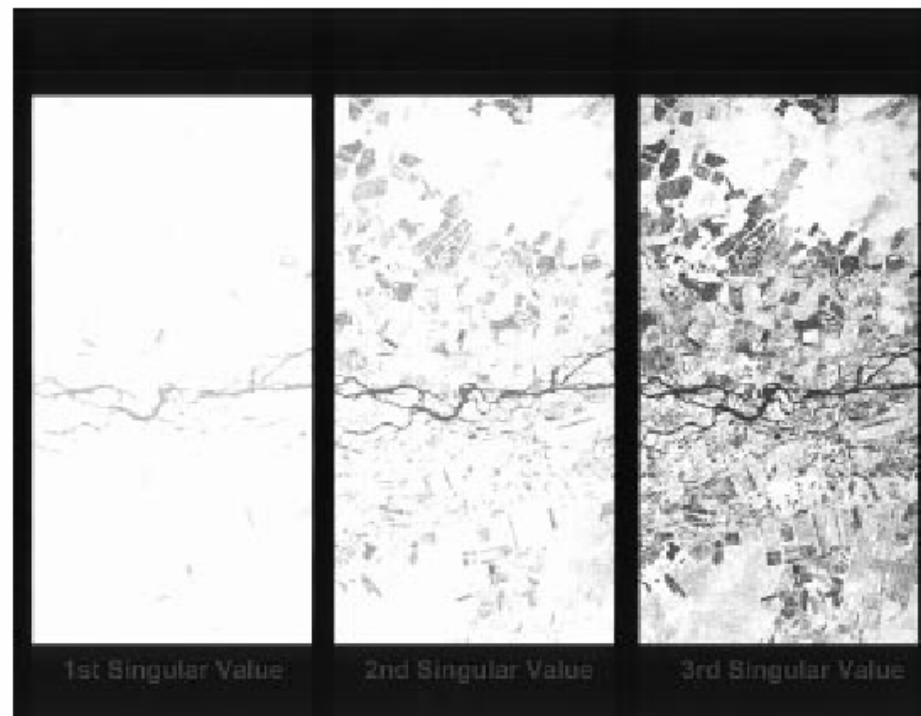


Fig. 7. Coherence maps of interferograms generated by using the optimum scattering mechanisms related to the first (left), second (middle), and third singular value (right).



Interpretation through a MODEL



Fig. 9. Three-dimensional representation of the height difference between effective phase scattering centers of the forested areas.



V. CONCLUSIONS AND PERSPECTIVES

- 1) **ALL** processing tools are now developed and available at CSL
- 2) **Need of DATA**
 - **Reliable acquisition plans**
 - **Future sensors** (RADARSAT-2, TerraSAR X, ALOS, SAOCOM,...)